CROSSDRO

Deliverable

D5.3 Projected changes in meteorological drought risk under future climate change scenarios

Christoph Menz

May 8, 2023

Contents

1 Introduction

In recent years Europe has experienced a unprecedented number of drought events. For example in 2003, 2010, 2013 and between 2015 and 2020 Europe was hit by exceptional dry conditions (Hanel et al., 2018; García-Herrera et al., 2019; Commission et al., 2021; Rakovec et al., 2022). These droughts had a strong impact on the agricultural sector, human health, surface and groundwater resources, the forest sector, and other parts of the socio-economic system and the environment. Due to variability of the climate system it is difficult to attribute singular drought events to anthropogenic warming. Furthermore, projections of future drought events are also associated with high uncertainties. However, to prompt mitigation measures and facilitate the development of adaptation measures to prevent and lessen the negative consequences of the anticipated changes in drought events, it is important to have a concise knowledge on historical and future evolution of droughts. According to the latest climate projections, drought impacts are expected to intensify in the future (Spinoni et al., 2018; Commission et al., 2020). In this report, we would like to extend on earlier studies on the impact of climate change on historical and future drought events.

2 Data and Methods

2.1 Climate Data

This report is based on two different climate dataset. Gridded observations of historical climate and Regional Climate Model (RCM) simulations of historical and future periods.

2.1.1 Climate Observations

We utilize the E-OBS v19.0e and v24.0e dataset (Cornes et al., 2018) as reference observation of the historical period. This dataset comprises daily temperature (minimum, mean and maximum) and precipitation observations for the period 1950 to 2018. It is based on in-situ weather station measurements that are interpolated to a regular geographical grid of $0.1°$ grid. The interpolation involves a stochastic component (to represent spatial correlation anomalies) to produce an ensemble of historical gridded climate observations. Within this report, we only use the ensemble mean fields as "best-guess" of the observed conditions. E-OBS is used within this report to assess the historical climate change signal, to evaluate the regional climate models and as reference dataset for bias adjustment of the RCMs. To further process the data, we performed an interpolation of E-OBS to a rotated pole grid at $0.11°$ horizontal resolution as used by the RCMs. Due to observational gaps in E-OBS v19.0e and v24.0*e* the whole European continent can not be covered fully. Therefore, we restrict our analysis only to areas where continuous observations of all four variables over the full time span (1950–2018) are available. The purple area in Figure 2.1 depicts the regions covered in our report. For analyzing the historical climate change we use E-OBS v24.0e, while we use the older Version v19.0e for bias adjustment and evaluation of our RCM ensemble.

2.1.2 Climate Model Simulations

To assess possible future changes in drought risk we utilize RCM simulations created within the CORDEX framework. These simulations were conducted by several research institutes within the EURO-CORDEX community (https://www.euro-cordex.net) for the predefined domain CORDEX-EUR11. This domain covers the European continent within the bounds shown in Figure 2.1 at a horizontal resolution of $0.11°$. RCMs simulate the atmospheric circulation for a limited domain at high spatial resolution. Due to the high spatial resolution RCMs capture the fine scale characteristics of precipitation and atmospheric conditions near complex orography and coastlines much better than their coarse Global Climate Model (GCM) counterparts. Hence, they are much more suitable when investigating future drought risk. The necessary information on the state of the atmosphere at the boundary of that domain is usually provided by coarse scale GCMs. Our RCM ensemble comprises 8 RCMs driven by 10 different GCMs. The GCMs simulations utilized were conducted within Coupled Model Intercomparison Project Phase 5 (CMIP5). Table 2.1 summarizes the RCM-GCM matrix (all RCM-GCM combinations) utilized in this report. In total
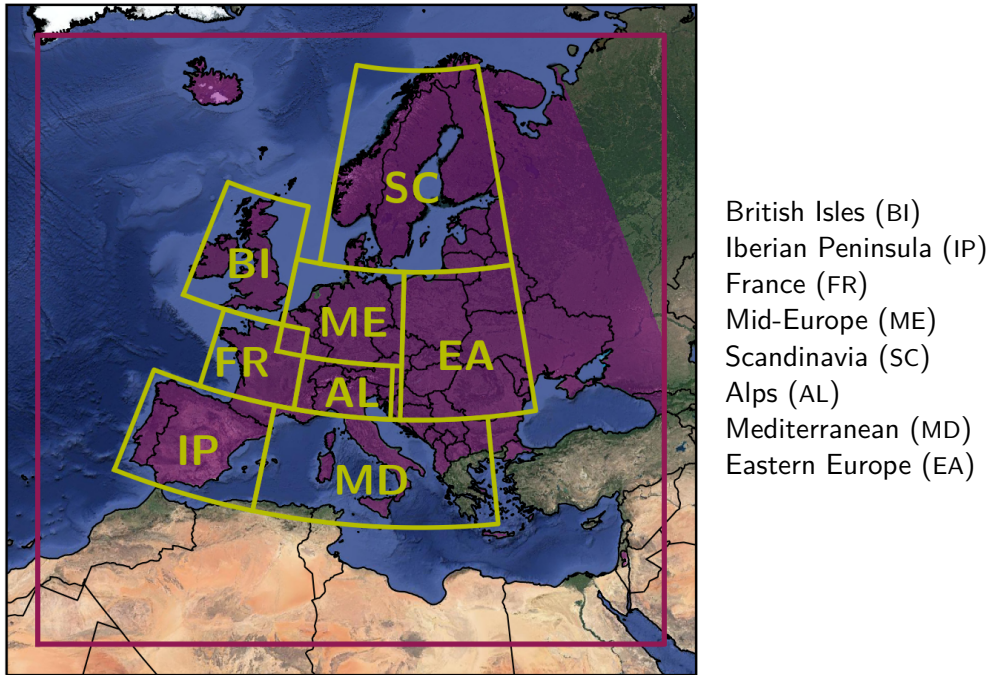
Figure 2.1: Domain definition subject to this report. The purple box represents the full modelling domain simulated by the RCM ensemble, i.e. the Coordinated Regional Climate Downscaling Experiment (CORDEX)-EUR11 domain. The purple area represents regions covered by this report, due to limitations in the data coverage of E-OBS v19.0e. Green boxes define sub-regions of Europe used for regional analysis. These regions are defined within the PRUDENCE project (Jens Hesselbjerg Christensen and O. B. Christensen, 2007).

our ensemble contains 39 simulations (RCM-GCM combinations including different realizations of a specific GCM and versions of RCM). The simulations cover the historical period and 3 future scenarios, represented by so called Representative Concentration Pathways (RCPs, van Vuuren et al., 2011). More specifically the ensemble covers 18 simulations under RCP 2.6, 17 simulations under RCP 4.5 and 37 simulations under RCP 8.5. The simulations for the historical period cover a time frame from 1971 to 2005 using observed greenhouse gas concentrations. Future projections start in 2006, using initial conditions from the last date of the historical simulations, and cover the whole 21st century until 2099 (HadGEM2-ES driven simulations) and 2100. Considering both historical simulations and future projections our ensemble covers a period of 1971 to 2100 in total. From the whole RCM ensemble we utilized daily temperature (minimum, mean and maximum) and precipitation for analysis in this report.

It is recognized in the scientific community, that the utilized CORDEX-EUR11 ensemble shows substantial biases in various variables. (Kotlarski et al., 2014). This bias prohibit its direct usage in climate change impact studies (Jens H. Christensen et al., 2008; Maraun, 2016), like this one. Therefore, we applied a state-of-the-art bias adjustment to the data and performed a comprehensive evaluation of the bias adjusted ensemble in Section 2.4.

GCM/RCM	CCLM	HIRHAM5	RACMO22E	RCA4	REMO2009	REMO2015	WRF331F	WRF361H
CanESM2	X					X		
CNRM-CM5	X	X	X	X		X		
EC-EARTH	X	X	X	X		X		X
CM5A-LR								
CM5A-MR				X			X	
MIROC5	X					X		
HadGEM2-ES	X	X	X	X		X		X
MPI-ESM-LR	X			X	X			X
NorESM1-M		X		X		X		
GFDL-ESM2G						X		

Table 2.1: Model matrix of RCMs and driving GCMs.

2.2 Climate Indices

In order to quantify the impact of climate change on drought events we employed different drought related climate variables and drought indices. The report focuses on meteorological droughts. Hence, droughts that are defined by meteorological variables or variables that define the state of the atmosphere.

Precipitation is the most important variable with respect to droughts, as it represents the primary influx of water into the hydrological cycle of a given region. A lack of precipitation can trigger a drought event. Therefore, our investigation on future drought risk will primarily rely on precipitation. A decrease in precipitation does not necessarily lead to an increased drought risk. Important aspects of precipitation that are related to drought risk are the seasonal (e.g., dry and wet season) and spatial distribution (e.g., local or large-scale events), duration of precipitation events (e.g., short convective or long-term cyclonic events), and cumulative amounts with respect to regional water demand (e.g., agricultural or ecological water use). Precipitation is frequently observed in weather stations and a standard output of climate models.

In addition to precipitation, evapotranspiration needs to be considered when analysing future drought risks. Besides runoff and infiltration, evapotranspiration is a major mechanism to extract water from surface. Evapotranspiration combines the two effects of surface evaporation and plant transpiration. Both effects are themselves highly complex. Evapotranspiration is rarely measured at weather stations and is usually not part of climate model outputs. However, there exist numerous methods to parameterize evapotranspiration, using environmental parameters like temperature and relative humidity. Most methods to calculate evapotranspiration do not consider actual available water and instead assume an infinite water source to evaporate from, therefore, overestimate evapotranspiration. Hence, these methods calculate only potential evapotranspiration values or the so-called atmospheric evaporative water demand. The methods to calculate evaporative water demand differ strongly in their complexity and the mechanisms and feedbacks considered to generate evapotranspiration. Choosing a specific method is usually

determined by the number and kind of environmental parameters at hand.

Due to the limited availability of parameters from the bias adjusted RCM ensemble (only temperature and precipitation are available) we choose to use Hargreaves method (Hargreaves and Samani, 1985) to calculate potential evapotranspiration. Hargreaves depends only on temperature and extra-terrestrial (top-of-the-atmosphere, TOA) radiation, hence can be easily calculated from the bias adjusted model outputs and latitude position of each grid cell. In presence of insufficient meteorological data, Hargreaves method is recommended by the Food and Agriculture Organization (FAO, (Allan et al., 1998)).

To characterize changes in drought events duration and frequency, we use three different indicators. These indicators are based on the absence of precipitation on consecutive days. For each indicator a dry day is considered a day with precipitation below $1.0\,\mathrm{mm/d}$. The following indicators for drought events were utilized:

1. The number of dry days (dry spell length), which is the total number of consecutive days with precipitation below $1.0\,\mathrm{mm/d}$. We only consider events of at least 7 consecutive dry days. The number of dry days is calculated per year or season.

2. The frequency of dry spells, which is the number of separate drought events per period, e.g., a year or a season. Two events are considered separate, if one or more days with precipitation of at least $1.0\,\mathrm{mm/d}$ separates them.

3. The longest drought event per period per year. Hence, the number of days of the longest dry episode for a given season (or the whole year) each year.

A intuitive drought definition based on the lack of precipitation alone, is not capturing the complexity of drought events and the multitude of impacts. For example, drought conditions can be also triggered by excessive evapotranspiration. In general the balance of precipitation and evapotranspiration, i.e., the climatic water balance, need to be considered simultaneously. Furthermore, the definition of a drought event should be defined on the average climate conditions of the region of interest. And finally, drought events can appear over different timescales at various magnitudes. To attribute these issues we utilized the Standardized Precipitation Evapotranspiration Index. The Standardized Precipitation Evapotranspiration Index (SPEI) was developed by Vicente-Serrano et al. (2010). It utilizes the climatic water balance:

$$P - PET, \tag{2.1}$$

with precipitation P and potential evapotranspiration PET to identify drought events on a monthly basis. In order to calculate the climatic water balance we estimated potential evapotranspiration using Hargreaves method (Hargreaves and Samani, 1985). In the following, we applied a sliding window sum filter on the monthly mean climatic water balance over $3, 6, 12,$ and 24 months. This way we can consider different types of meteorological droughts, from short term (3 months, e.g., representing shortage of surface water bodies) to long term (24 months, e.g., representing soil water deficit or groundwater shortage) droughts. The resulting time series was fitted to a Pearson Type III distribution over a reference period of 1971–2000 (model simulations were fitted over the corresponding time frame in the historical period) for each month of the year separately. Each value of the filtered water balance can then be expressed in terms of the cumulative distribution function (i.e., probability of being less or equal a given water balance value). The final SPEI value is calculated as the relative difference in terms of the standard deviation of the distribution. SPEI is estimated for each grid box separately.

2.3 Estimation of Statistical Parameters

It is known, that simulations from RCMs exhibit considerable uncertainties from various sources. When estimating statistical parameters one has to consider these different sources and their contribution to the overall uncertainty. In general we assume that the uncertainty is represented by the time series variability, i.e., we use uncertainty synonym to variability. In this report we consider 3 different sources of uncertainty:

- Natural uncertainty, represented by the variation in the time series of a single model simulation.

- RCM uncertainty, represented by the variation between different RCMs.

- GCM uncertainty, represented by the variation between different driving GCMs.

Furthermore, we considered different realizations of a single GCM and different versions of a single RCM as a possible source of uncertainty. However, since most GCM-RCM combination use only a single realization/version we assume this contribution to be small compared to the other sources. So in general the ensemble can be structured in 5 different levels associated to the uncertainty: time series (representing natural uncertainty), RCM, version of the RCM, GCM and realization of that GCM. Due to the nature of the modeled system and the structure of the ensemble we have to consider correlations between the different sources and implement a proper uncertainty propagation. Therefore, we applied a bootstrapping re-sampling (Efron, 1979; Efron and Tibshirani, 1986) to estimate statistical parameters. The bootstrapping re-sampling draws random elements from the original ensemble to build a artificial ensemble of same size and structure. The structure is maintained by performing independent draw on each level of the ensemble (i.e., GCM, realization, RCM, version and time series level). Preserving the structure is important, since we are dealing with an unbalanced ensemble, e.g., some RCMs contribute with 7 simulations to the ensemble while others only with 1. The procedure of randomly drawing a new ensemble is repeated multiple times to generate multiple artificial ensembles.

In the following, the statistical parameter is calculated on each ensemble and statistical significance can be estimated based on the spread over the artificial ensembles. As re-sampling and estimation of statistical parameters is a computational demanding task, we choose to draw 1000 different artificial ensembles, which is a trade-off of statistical accuracy (law of large numbers) and computing time. Throughout the report we will use a 30 % significance level (15 % lower and 85 % upper bound). We did not consider the RCP scenarios as a source of uncertainty, since we wanted to show the results depending on different concentration pathways.

2.4 Bias Adjustment

Global and regional climate models are abstract approximations of the real-world earth system. Due to our imperfect knowledge of the earth system and the inherent model deficiencies it is well-know that these models, and in particular the models of our RCM ensemble, show a systematic deviation from observed historical climate (see for example Kotlarski et al., 2014). This deviation is called a model bias and it prohibit the direct usage of climate model simulations in climate change impact studies (Jens H. Christensen et al., 2008; Maraun, 2016).

As the upper panel of Figure 2.2 demonstrates, our RCM ensemble underestimates temperature and overestimates precipitation over large areas of Europe. The largest biases in both variables appear over the Alps and along the Norwegian coast. Cold bias can be as large as $-3\,\mathrm{K}$ in isolated areas while precipitation shows a wide spread overestimation above $0.5\,\mathrm{mm/d}$. The cold and wet bias can be assumed to be linked as higher precipitation leads to higher water availability at the surface which increases evaporative cooling. Biases in primary variables like precipitation can also propagate into derived climate indices like dry spell length. As can be seen in the upper right map of Figure 2.2, the overestimation of precipitation is associated with a significant underestimation of drought spell length. Especially the bias in precipitation and drought spell length prohibit the utilization of the raw RCM ensemble in our further analysis.

Statistical measures of model output statistics (MOS) (Glahn and Lowry, 1972) were developed to reduce the bias. These methods are called bias adjustment methods. In the last 20 years various methods of different complexity where developed and applied to various climate model ensembles (Dosio and Paruolo, 2011; Teutschbein and Seibert, 2012; Hempel et al., 2013; Wilcke et al., 2013; Lange, 2017). To overcome the issue of model biases in this report we employ a state-of-the-art bias adjustment method called ISIMIP3BASD (Lange, 2019), developed within the The Inter-Sectoral Impact Model Intercomparison Project Phase 3 (ISIMIP3, BASD - Bias Adjustment and Statistical Downscaling). The ISIMIP3BASD method utilizes quantile mapping approach to adjust model biases. Depending on the user specification, the method uses a parametric or non-parametric quantile mapping. In general quantile mapping tries to map the quantiles of a modeled distribution (based on the time series of a single grid box) with a observed distribution. This mapping is called a *transfer function*. In order to apply the bias adjustment, the transfer function has to be compiled, using observations and model simulations of the same period, usually a historical period of 30 years length sharing the same climatic conditions. Parametric quantile mapping tries to fit the empirical distribution to a pre-defined parametric distribution, while non-parametric quantile mapping relies on the empirical distribution as is. The advantage of the parametric approach is a better representation of distribution tails (extremes), however it requires a sufficient sampling of the empirical distribution and heavily relies on the correct choice of distribution type. On the other hand a non-parametric approach is usually more robust but can perform poorly when adjusting values at the tails of the distribution. One advantage of the ISIMIP3BASD method is its ability to preserve trends in all quantiles of a given variable. This is necessary, since quantile mapping approaches are known to artificially disturb the change signal (Dosio and Paruolo, 2011; Cannon et al., 2015). In this report we only preserve temperature trends. Due to the high variability of precipitation it was decided not to preserve its trend. The bias adjustment was applied to each model simulation (RCM/GCM combination) separately. For each model the ISIMIP3BASD transfer function was compiled for the historical simulation period 1971–2000 using E-OBS v19.0e as reference observation. The transfer function can then be applied to model simulations of a future period. Within this report, bias adjustment was only applied to the primary variables temperature and precipitation. All derived variables were calculated using the primary variables after bias adjustment. Hence, derived variables were not directly bias adjusted.

Figure 2.2 gives a brief overview of the evaluation of the model ensemble before and after bias adjustment. As stated before prior to the bias adjustment, the ensemble was characterized by a large scale overestimation of precipitation and underestimation of temperature. Consequently dry spells were underestimated across the whole European continent. Hence, a utilization of the biased ensemble to investigate drought effects is not advised. After bias adjustment most areas

show considerably lower biases for temperature and precipitation below statistical significance (p< 0.3). Only small areas in France, along the Pyrenees and in Italy reveal a statistical significant underestimation of precipitation. Although, the bias adjustment does only adjust the bias of temperature and precipitation, also derived variables like dry spell length show a considerable reduction in bias (see Figure 2.2). Most areas show no statistical significant bias. Only small areas along the continental Atlantic coast, over the British Isles and the Mediterranean show a small and significant underestimation. These areas coincide with the areas of largest bias prior the bias adjustment.

In more detail, Table 2.2 and 2.3 summarize the temperature and precipitation bias after bias adjustment for various different seasons and domains defined in Figure 2.1. Median temperature bias is below $0.1\,^{\circ}$C for most domains and seasons. The total temperature bias range varies between $-0.95\,^{\circ}$C and $+0.95\,^{\circ}$C (5 to 95 percentile). The singular largest bias can be observed for winter season (DJF) over the Mediterranean domain. While the largest median bias across all domains can be observed in summer (JJA). For the majority of domains our bias adjusted RCM ensembles shows a cold bias in autumn and winter (SON and DJF) and a warm bias in spring and summer (MAM and JJA). Considering the absolute numbers, bias of the individual models was reduced considerably. Persistent biases are restricted to single models, seasons and domains. Precipitation bias is also considerably reduced (see Table 2.3) with median values mostly below 0.1 mm/d and bias ranges between -0.43 mm/d and 0.27 mm/d across all domains and seasons. In contrast to the strong wet bias of the original ensemble our RCM ensemble shows a small dry bias after bias adjustment. However, this dry bias is around one order of magnitude below the wet bias prior to the bias adjustment. Therefore, we assume, that the bias adjusted ensemble to be suitable for further analysis regarding future drought risk.

Despite the small overall biases found after bias adjustment it needs to be kept in mind, that the bias adjustment method applied, assumes the bias to be constant in time and did not consider any feedbacks or thresholds in the climate system. Hence it might be possible, that the bias adjusted RCM ensemble still underestimates regional changes (Bellprat et al., 2013). On the other hand it was shown by Boberg and Jens H. Christensen (2012) that temperature changes in the Mediterranean might be overestimated by the models already. Along with the small persistent bias found in out bias adjusted RCM ensemble this needs to be considered when analyzing future drought risk.

Domain	Annual	DJF	MAM	JJA	SON
BI	$+0.03^{+0.25}_{-0.17}$	$+0.02^{+0.47}_{-0.39}$	$+0.07^{+0.36}_{-0.22}$	$+0.04^{+0.36}_{-0.29}$	$+0.01^{+0.31}_{-0.28}$
IP	$+0.04^{+0.27}_{-0.19}$	$-0.02^{+0.34}_{-0.39}$	$+0.14^{+0.51}_{-0.24}$	$+0.15^{+0.52}_{-0.21}$	$-0.04^{+0.31}_{-0.40}$
FR	$+0.05^{+0.30}_{-0.21}$	$-0.01^{+0.51}_{-0.53}$	$+0.12^{+0.47}_{-0.24}$	$+0.14^{+0.55}_{-0.26}$	$-0.00^{+0.36}_{-0.36}$
ME	$+0.04^{+0.32}_{-0.27}$	$-0.06^{+0.68}_{-0.74}$	$+0.08^{+0.50}_{-0.35}$	$+0.11^{+0.51}_{-0.32}$	$-0.01^{+0.36}_{-0.38}$
SC	$-0.00^{+0.38}_{-0.39}$	$+0.00^{+0.95}_{-0.95}$	$-0.02^{+0.45}_{-0.55}$	$+0.04^{+0.42}_{-0.34}$	$-0.05^{+0.47}_{-0.50}$
AL	$+0.03^{+0.27}_{-0.22}$	$-0.09^{+0.40}_{-0.57}$	$+0.10^{+0.50}_{-0.28}$	$+0.13^{+0.52}_{-0.22}$	$-0.03^{+0.33}_{-0.39}$
MD	$-0.21^{+0.00}_{-0.43}$	$-0.45^{-0.06}_{-0.83}$	$-0.09^{+0.30}_{-0.44}$	$-0.07^{+0.29}_{-0.42}$	$-0.26^{+0.08}_{-0.60}$
EA	$+0.00^{+0.33}_{-0.32}$	$-0.14^{+0.68}_{-0.88}$	$+0.01^{+0.55}_{-0.49}$	$+0.09^{+0.46}_{-0.27}$	$+0.04^{+0.42}_{-0.37}$

Table 2.2: Ensemble median temperature bias averaged for specific domains defined in Figure 2.1. Sub- and superscripts represent the 5 and 95 percentile of the ensemble respectively. The bias was estimated for the period 1971–2000 using E-OBS v19.0e as reference.

Temperature Precipitation Dry Spell Length

Temperature Bias [K]

-3 -2 -1 0 1 2 3

Precipitation Bias [mm/d]

-0.7 -0.6 -0.5 -0.4 -0.3 -0.2 -0.1 -0.0 0.1 0.2 0.3 0.4 0.5 0.6 0.7

Number of Dry Days Bias [d]

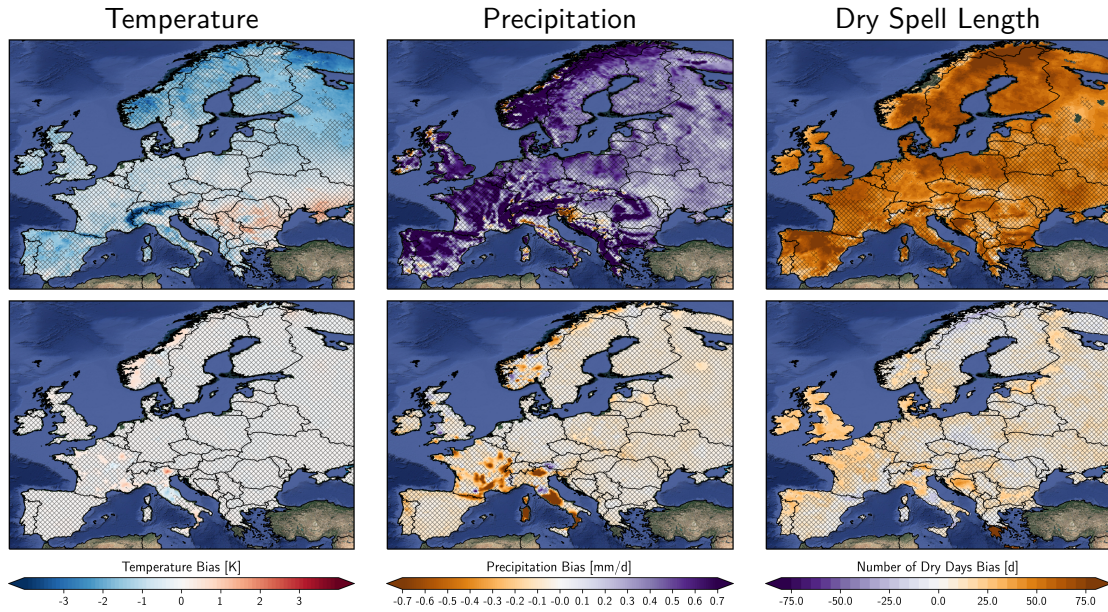-75.0 -50.0 -25.0 0.0 25.0 50.0 75.0

Figure 2.2: Ensemble mean of annual mean bias of temperature (left), precipitation (center) and dry spell length (right). The upper row represents our RCM ensemble prior to the bias adjustment, while the lower row represents the ensemble after bias adjustment. The bias was estimated for the period 1971–2000 using E-OBS v19.0e as reference. Shaded areas depict regions with bias outside a 10 % significance level, which are not considered statistical significant.

Domain	Annual	DJF	MAM	JJA	SON
BI	$-0.05^{+0.05}_{-0.16}$	$-0.04^{+0.22}_{-0.32}$	$-0.04^{+0.16}_{-0.23}$	$-0.03^{+0.18}_{-0.25}$	$-0.08^{+0.18}_{-0.32}$
IP	$-0.07^{+0.03}_{-0.17}$	$-0.12^{+0.19}_{-0.43}$	$-0.05^{+0.12}_{-0.24}$	$-0.06^{+0.05}_{-0.18}$	$-0.03^{+0.19}_{-0.23}$
FR	$-0.06^{+0.05}_{-0.16}$	$-0.06^{+0.18}_{-0.29}$	$-0.06^{+0.16}_{-0.28}$	$-0.05^{+0.13}_{-0.22}$	$-0.06^{+0.21}_{-0.32}$
ME	$-0.03^{+0.07}_{-0.13}$	$-0.01^{+0.21}_{-0.19}$	$-0.05^{+0.11}_{-0.22}$	$-0.05^{+0.12}_{-0.22}$	$-0.02^{+0.17}_{-0.20}$
SC	$-0.04^{+0.03}_{-0.10}$	$-0.01^{+0.15}_{-0.16}$	$-0.03^{+0.08}_{-0.13}$	$-0.03^{+0.14}_{-0.20}$	$-0.08^{+0.05}_{-0.20}$
AL	$-0.10^{+0.02}_{-0.22}$	$-0.11^{+0.12}_{-0.34}$	$-0.11^{+0.12}_{-0.35}$	$-0.11^{+0.08}_{-0.33}$	$-0.05^{+0.27}_{-0.38}$
MD	$-0.01^{+0.08}_{-0.09}$	$-0.04^{+0.15}_{-0.24}$	$-0.03^{+0.10}_{-0.17}$	$+0.04^{+0.17}_{-0.11}$	$+0.00^{+0.18}_{-0.16}$
EA	$-0.04^{+0.03}_{-0.11}$	$-0.03^{+0.06}_{-0.11}$	$-0.05^{+0.04}_{-0.15}$	$-0.06^{+0.12}_{-0.24}$	$-0.04^{+0.12}_{-0.19}$

Table 2.3: Same as 2.2 for precipitation.

3 Observed Changes

In recent decades Europe already observed a significant change in the climatic conditions. As shown in Figure 3.1 annual mean temperature has increased throughout the whole continent by around $1\,^\circ$C since the beginning of the 21st century (2001–2020 relative to 1981–2000). The dryer eastern part of Europe and the Mediterranean experienced a slightly higher increase compared to the rest of the continent. Due to the increased temperature, also annual averaged potential evapotranspiration has increased significantly between $0.1\,\mathrm{mm/d}$ and $0.2\,\mathrm{mm/d}$. Both temperature and evapotranspiration changes are statistical significant above $30\,\%$ significance level. On the other hand, no clear change for precipitation could be observed. Precipitation increase and decrease was observed heterogeneously and for most of Europe below statistical significance level. Most prominent decreases were observed over western Germany and eastern France, while over southern Italy and the Balkans precipitation decreased.

The changes in temperature and precipitation are directly reflected in changed drought conditions. As can be seen in Figure 3.2, especially Central Europe experienced a significant increase in number of drought days. Also along the Poland-Czech-Slovakia boarder and over large parts of Eastern Europe a strong increase of around one week (7 days) was observed. These areas represent major agricultural areas but also major cities and industry centers like metropolitan Paris, Rhine-Ruhr metropolitan region and Upper Silesian metropolitan area. These changes are reflected in the number of droughts observed in the 21$^{\mathrm{st}}$ century, affecting not only the agricultural sector but also human health, surface and groundwater resources and forestry. On the other hand, the already dry Mediterranean did not show a statistical significant change in number of drought days. Southern Italy and the Balkans especially show strong decrease in the number of drought days.

According to the dry spell frequency only small areas with statistical significant changes were observed (see Figure 3.2). For example the Upper Silesian metropolitan region, central Ukraine and south-western Iberian Peninsula, showed an increase in dry spell frequency between 1 and 2 events per year. Similar to the number of dry days, an increase in dry spell frequency could be observed over some parts of the Balkans and southern Italy. As the changes in dry spell frequency suggests, the changes in number of dry days over the Upper Silesian metropolitan area and eastern Europe are mostly related to the development of additional drought events over the year, rather than a prolongation of existing drought periods. The latter is true for the observed increase in number of dry days over Germany and France. Regarding the maximum number of consecutive dry days (see the lower panel in Figure 3.2) no statistical significant change can be observed. The predominant increase of Central European regions agrees with an increase in drought duration.

With respect to the environmental and socioeconomic impacts also the seasonal distribution of droughts are important. Therefore, we show in Figure 3.3 the changes in the number of dry days for the four seasons winter (DJF), spring (MAM), summer (JJA) and autumn (SON). The figure reveals that the significant increase over eastern France and western Germany is mostly observed in spring and autumn. Especially spring drought are frequently happen in this
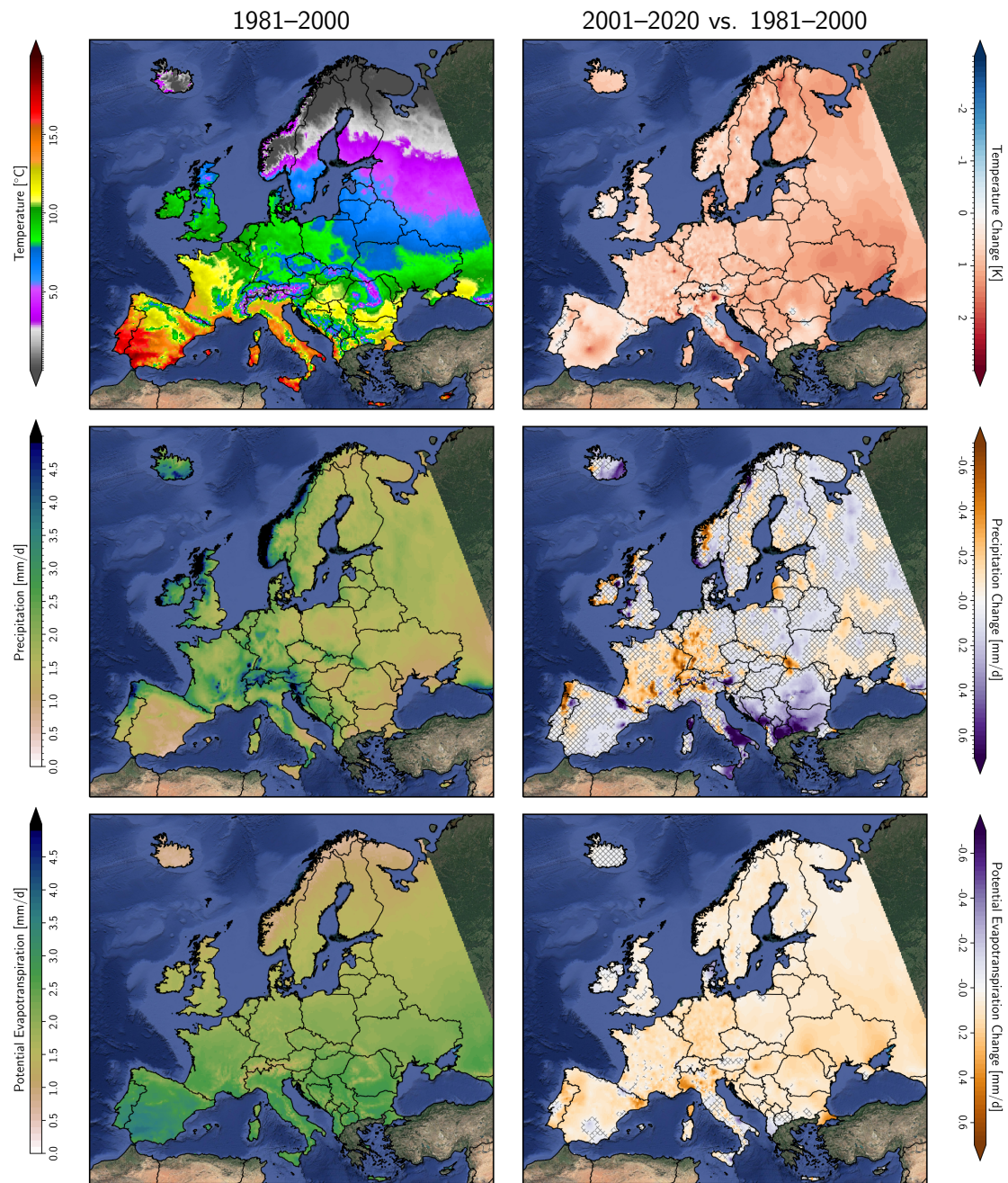
Figure 3.1: Annual mean temperature (top), precipitation (center) and potential evapotranspiration (bottom) observations (left, 1981–2000) and changes (right, 2001–2020 vs. 1981–2000) according to E-OBS v24.0e. Shaded area in the change plot represents grid cells with changes below significance level of 30 %.

areas putting pressure on agriculture plants in their early development phase. An increased number of drought days together with increased evapotranspiration posses an increased pressure on the agriculture sector, leading to higher water stress levels in plants and earlier phenological
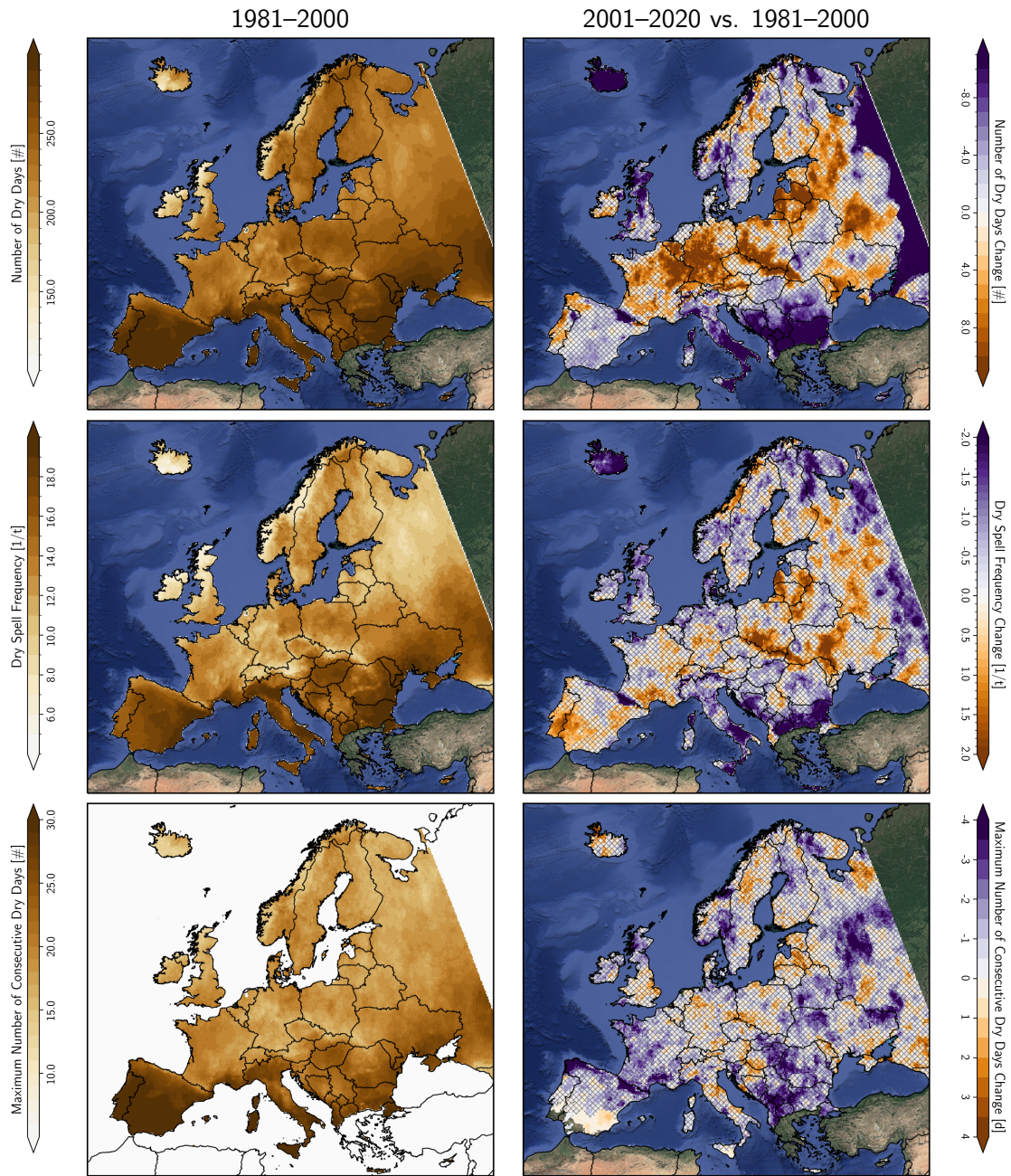
Figure 3.2: Same as Figure 3.1 for the number of dry days (top), dry spell frequency (center) and the longest dry spell period (bottom).

development. Furthermore, the number of summer dry days has increased over agricultural areas of the Upper Silesian area and some parts of eastern Europe, like central Ukraine, as well.

In addition to the changes in dry day frequency we also analyzed historical change of SPEI at different time scales in Figure 3.4. It confirms the drying trend of major parts of central Europe. This change is driven by the decrease in precipitation and an increase in evapotranspiration, due
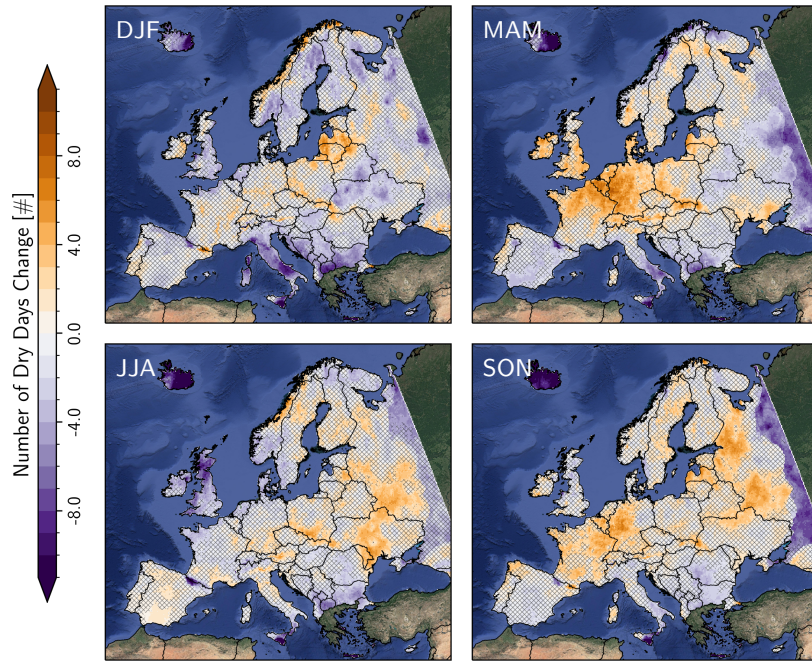
Figure 3.3: Change in number of dry days for 2001–2020 compared to 1981–2000 for winter (DJF), spring (MAM), summer (JJA) and autumn SON.
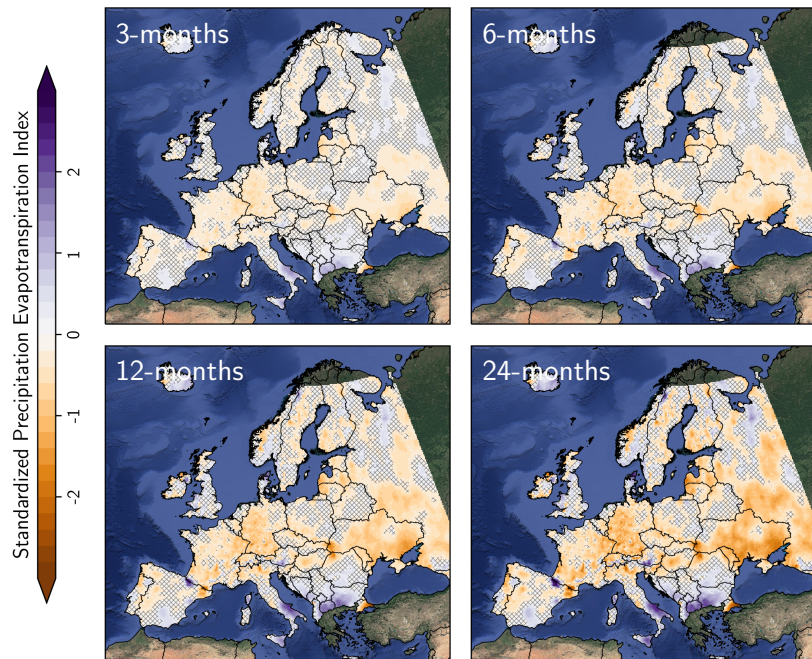
Figure 3.4: Observed change of SPEI for 4 different time-scales. Changes are calculated for 2001–2020 with respect to 1981–2000 based on E-OBS v24.0e.

to increased temperatures. A decreasing SPEI is statistical significant for most parts of France, Germany and the Ukraine. An increase can only be observed over the Balkans and southern Italy. However, most changes are quite small, within a -1 to $+1$ range. According to the different time scales of SPEI, lowest changes are observed for 3-month scale, i.e., systems quickly responding to changes in water availability, like surface water bodies or agriculture. For longer time scales also the changes increase. Hence, the slower the system response to water shortage the stronger the change. In other words long-term drought events showed a stronger increase in intensity than short term droughts. This could be expected as on driving factor is the slow but steady increase on temperature and evapotranspiration.

4 Future Projections

To evaluate anticipated future changes in drought events we utilize a high resolution and bias adjusted RCM ensemble developed within the CORDEX-EUR11 framework.

4.1 Projected changes in temperature and precipitation

Figure 4.1 shows the anticipated temperature and precipitation change averaged over the European continent as simulated by the RCMs under 3 different RCPs scenarios until 2100 relative to 1981–2010. Temperatures are expected to increase between $1\,\mathrm{K}$ and $4\,\mathrm{K}$ until the end of the 21$^{\text{st}}$ century, depending on the RCP scenario. These changes are statistical significant at the 30 % significance level for every scenario. Hence, the already observed temperature increase (see Figure 3.1) is expected to continue and intensify, even under the most ambitious greenhouse gas concentration target. In contrast European averaged precipitation changes are below statistical significance. However, there is a tendency towards an increase of up to $1\,\mathrm{mm/d}$. These findings are in line with the already observed changes, where large temporal variability and spatial heterogeneity prohibit a clear picture for whole Europe. Compared to the changes in temperature no significant difference between the RCP scenarios can be observed. The different box plot ranges are due to the larger ensemble size for RCP 8.5.

Besides the general temperature and precipitation trend, also spatial and seasonal distribution of the anticipated changes are important. Therefore, Figure 4.2 and 4.3 present maps of changes for each season for the end of the 21$^{\text{st}}$ century under the highest greenhouse gas concentration scenario RCP 8.5. According to Figure 4.2 the temperature increase is mostly homogeneous across Europe. Slight seasonal differences can be seen in winter (DJF) and summer (JJA) season. With winter season anticipating stronger increase in the north-eastern part of Europe compared to the rest of the continent and summer season anticipating stronger increase in the Mediterranean area. The stronger temperature increase over north-eastern Europe in winter could be explained by a weakening of the Siberian high (Gong and Ho, 2002). However, there is a controversy in the scientific community about a possible weakening of the Siberian high as it is not consistently projected by recent GCMs (Li and Gao, 2015), instead an increase in inter-annual variability is projected. On the other hand, the stronger temperature increase in summer over the Mediterranean is most likely associated with the northward shift of the Hadley cell, leading to shift of the subtropical high pressure system over northern Africa towards the Mediterranean (MedECC, 2020). In spring (MAM) and autumn (SON) the magnitude of these spatial patterns are considerable smaller. In general throughout the seasons a smaller increase in temperature are projected over central European countries, while stronger increase is found over mountainous areas like the Alps. With respect to plant growth and future surface and subsurface water availability changes in autumn, winter and spring are important, as especially in central Europe groundwater resources are refilled in SON and DJF and started depleting in MAM. Due to increased temperatures it is expected, that plant development will start earlier in
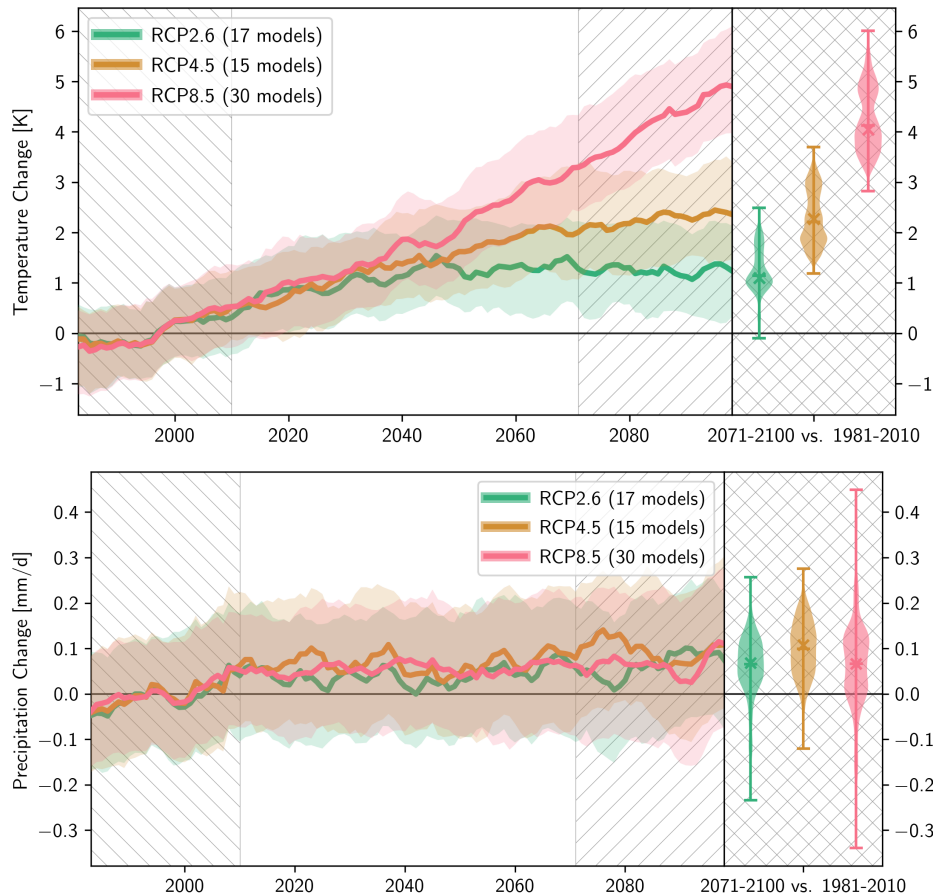
17

Figure 4.1: Future development of 2 m temperature (top) and precipitation (bottom) averaged over European continent based on a bias adjusted regional climate model ensemble. Three different RCPs scenarios are shown (RCP 2.6, RCP 4.5 and RCP 8.5). Solid line represents the ensemble median while the colored shaded area shows the ensemble spread of the respective RCP, defined by the 15th and 85th percentile. Percentiles are estimated using a bootstrapping re-sampling drawing 1000 samples.

the year, effectively reducing the period to refill the surface and subsurface water bodies during dormancy period. Higher temperatures are dangerous in particular, since they will directly affect the severity of drought events (e.g., through higher evapotranspiration).

Similar to already observed changes (see Figure 3.1) also the anticipated future changes in precipitation show a strong heterogeneity, as can be seen in Figure 4.3. A dominant pattern of precipitation change observed in every season is a south-north gradient, with decreasing precipitation in the south and increasing precipitation in the north. The area of decreasing precipitation propagates northward towards summer and southwards towards winter season. Hence, largest areas with decreasing precipitation can be seen in summer, covering major parts of central and eastern Europe and the Mediterranean. On the other hand, largest areas with increasing precipitation can be found in winter, covering whole central and eastern Europe. Throughout the year only Scandinavia shows a consistent increase in precipitation over all seasons up to 0.6 mm/d, while Iberian Peninsula and Italy shows a consistent decrease up to −0.6 mm/d.
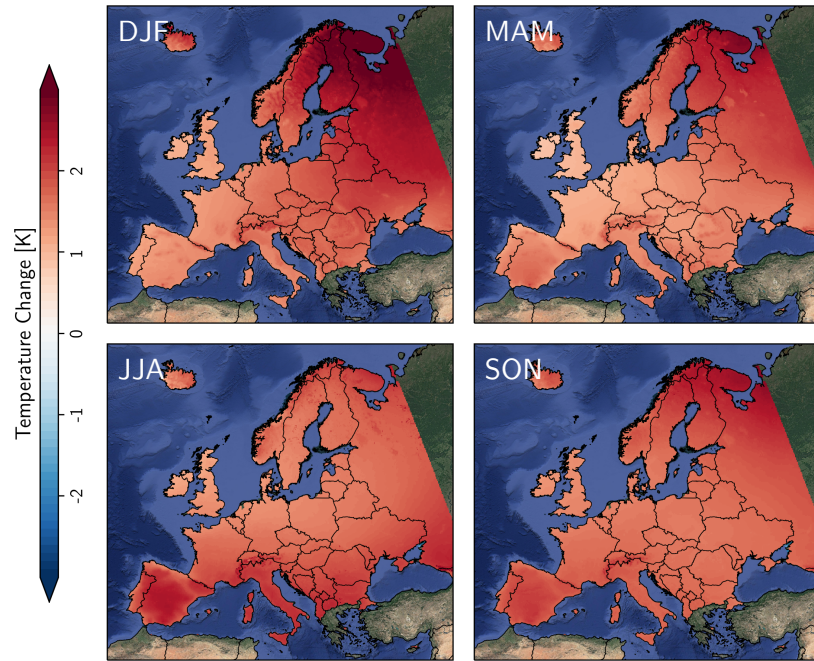
Figure 4.2: Spatial distribution of temperature changes in 2071–2100 compared to 1981–2010 for each season. Projections are based on the bias adjusted RCM ensemble for CORDEX-EUR11 following the RCP 8.5 scenario. Shaded areas represent change signals below a 30 % significance level, hence regions without statistical significant changes.

The decrease in precipitation in southern Europe is in line with the northward shift of the subtropical high pressure belt (as part of the Hadley cell) under climate change, as it will shift the northern storm track towards Scandinavia and the associated subsidence will prevent local convection. Compared to the observed changes over the last decades (see Figure 3.1), the changes in precipitation show a different pattern, especially over Mediterranean. However, the projected changes of the RCMs are in line with physical reasoning (northward shift of Hadley cell) and findings in other studies (see for example Jens Hesselbjerg Christensen and O. B. Christensen, 2007; Jacob et al., 2014). It is expected, that the decrease in precipitation over Mediterranean together with increased temperatures will put additional pressure on the agricultural sector in the Mediterranean countries. Besides intensifying droughts by extending the prolongation of drought events, reduced precipitation can also reduce recuperation after a drought event.

Due to the homogeneous increase in temperature also potential evapotranspiration is expected to increase throughout Europe, as can be seen in Figure 4.4. The strongest increase can be seen in the summer season for southern Europe. As expected earlier this will directly affect the severity of drought events in this already vulnerable region. As evapotranspiration depends on absolut temperature, a comparable temperature increase in winter season (see Figure 4.2) leads to a fairly low evapotranspiration increase, due to the lower absolute temperatures. This also explains the higher evapotranspiration change in the southern parts of Europe throughout the seasons. Except for winter season, it should be expected, that the increase in precipitation (see Figure 4.3) will be overcompensated by the decrease in evapotranspiration, effectively leading to less available water in most of European regions. All three parameters evaluated thus far
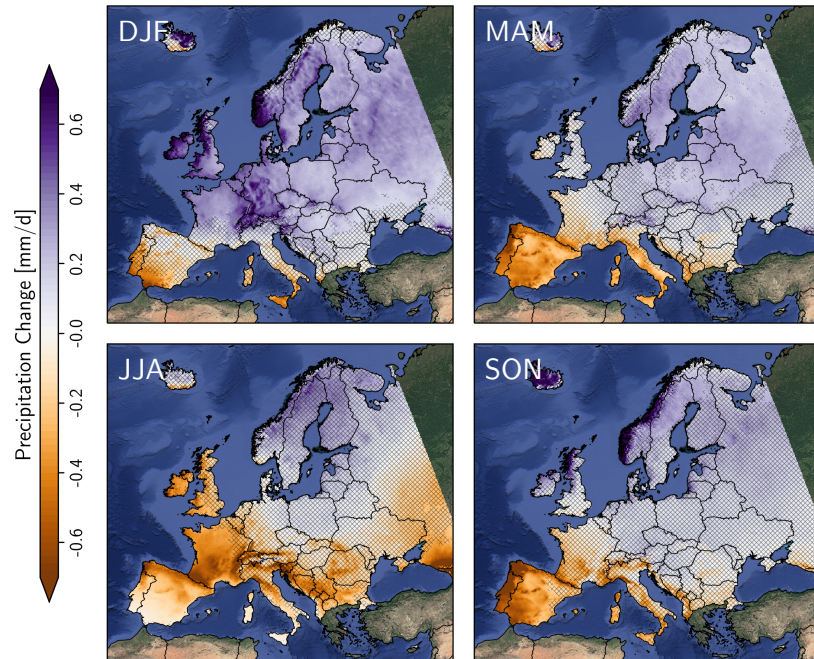
Figure 4.3: Same as Figure 4.2 for precipitation.

(temperature, precipitation and evapotranspiration) point towards an intensification of drought events and reduced recuperation after a drought event, putting additional pressure especially on Europe's agricultural sector to adapt to the anticipated consequences of climate change. In the following we will have a closer look into the drought changes in terms of drought duration and frequency.

4.2 Projected changes in drought duration and frequency

As seen in Figure 4.1 and 4.3 precipitation changes are highly variable in space and time. It can be expected, that these patterns are also resembled in the projected changes of indicators related to the length and frequency of drought events. Figure 4.5 presents the changes in number of dry days in 2071–2100 relative to 1981–2010 averaged over several regions of Europe, defined in Figure 2.1, for all three greenhouse gas concentration scenarios. In general, the projections do not show a significant change in the number of dry days for most regions and RCP scenarios. A statistical significant increase is projected for the southern domains (IP and MD) and under moderate and high concentration scenarios (RCP 4.5 and RCP 8.5). These changes are in line with the precipitation decrease anticipated for the Mediterranean. On the other hand, the projections don't show a significant decrease in number of dry days for the northern parts of Europe, despite these are projected to become wetter. Only a slight tendency to decrease is anticipated over SC in winter (DJF). For this reason we conclude, that the precipitation increase over northern Europe is due to an intensification of precipitation events and not due an increased number of wet days. The most significant changes in number of dry days can be observed in summer (JJA) season, with a median increase of around 5 dry days over most regions under RCP 8.5. For
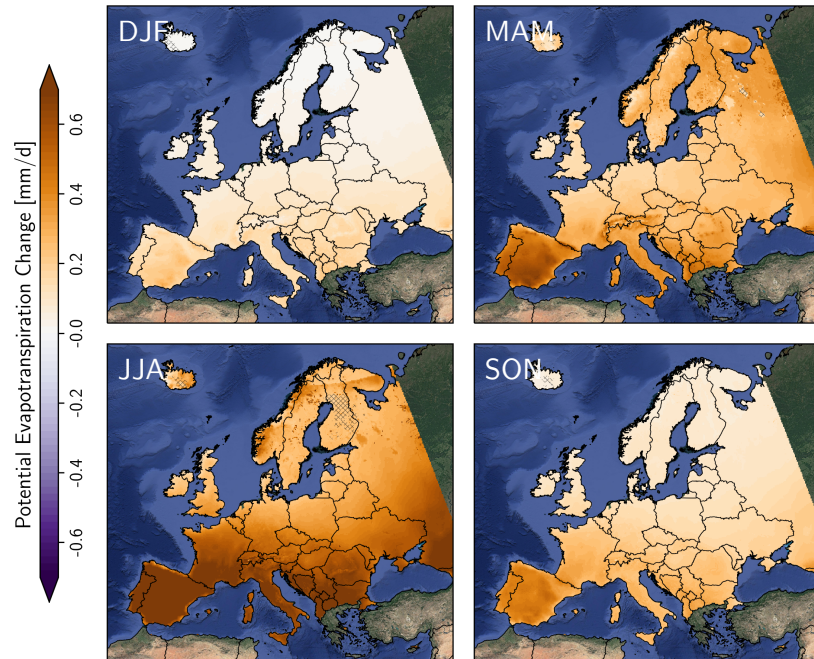
Figure 4.4: Same as Figure 4.2 for potential evapotranspiration based on Hargreaves method (Hargreaves and Samani, 1985).

spring (MAM) and autumn (SON) statistical significant changes are projected for FR, AL, IP and MD. For winter season only the Mediterranean (IP and MD) show statistical significant increase. Throughout all seasons and regions the ensemble does not project a statistical significant change for RCP 2.6. Similar changes can also be observed for the maximum number of consecutive dry days (not shown). Together with the anticipated temperature and precipitation changes, these finding further support the observation, that the Mediterranean area will be hit the hardest by climate change in terms of drought events, compared to other European regions.

The changes in number of dry days are also resembled in the changes of dry spell frequency (see Figure 4.6). The only difference can be seen in the summer months for IP and MD, where no change or even a decrease is projected. However, this can be explained by the already high number of dry days in summer in both regions (around 90 % of the days are dry days within 1981–2010). Additional dry days will lead in merging separated drought events, effectively decreasing the frequency of dry spells. Hence, these regions will observe less drought events but of much longer duration. Hence, reducing or removing the recovery period between drought events. The strongest change is anticipated for FR, where the ensemble projections show an median increase of one additional drought event every 1 to 2 years for spring, summer and autumn season. Together with increased temperature this will have a huge impact on the agriculture sector (e.g., vineyards). A similar increase, but less in magnitude, can be observed for AL. Furthermore, also other regions of central Europe show a significant increase in dry spell frequency in summer season.

According to our ensemble projections future climate change will be associated with a small increase in dry spell length and number of droughts per year (see Figure 4.5 and Figure 4.6). When developing adaptation measures like insurance products for agriculture it is also important
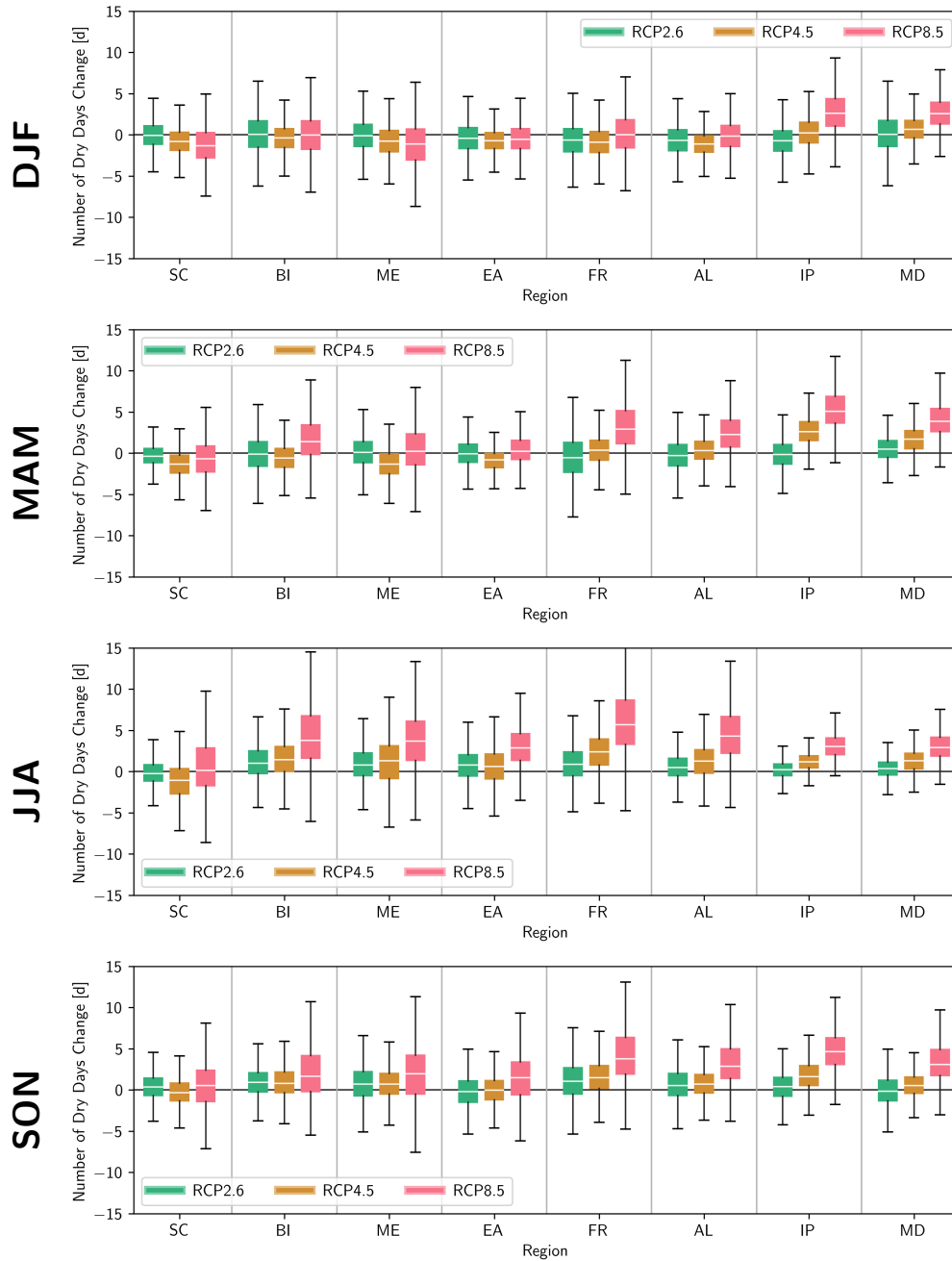
Figure 4.5: Change in number of dry days for the period 2071–2100 relative to the reference period 1981–2010 as simulated by the bias adjusted CORDEX-EUR11 ensemble following 3 different greenhouse gas concentration scenarios (RCP 2.6, RCP 4.5 and RCP 8.5). The boxes represent the ensemble spread of the area averaged changes for the 8 domains defined in Figure 2.1.

to know how the probability of rare drought events changes under future climate change. Therefore, Figure 4.7 shows the length of drought events under different global warming levels for 5
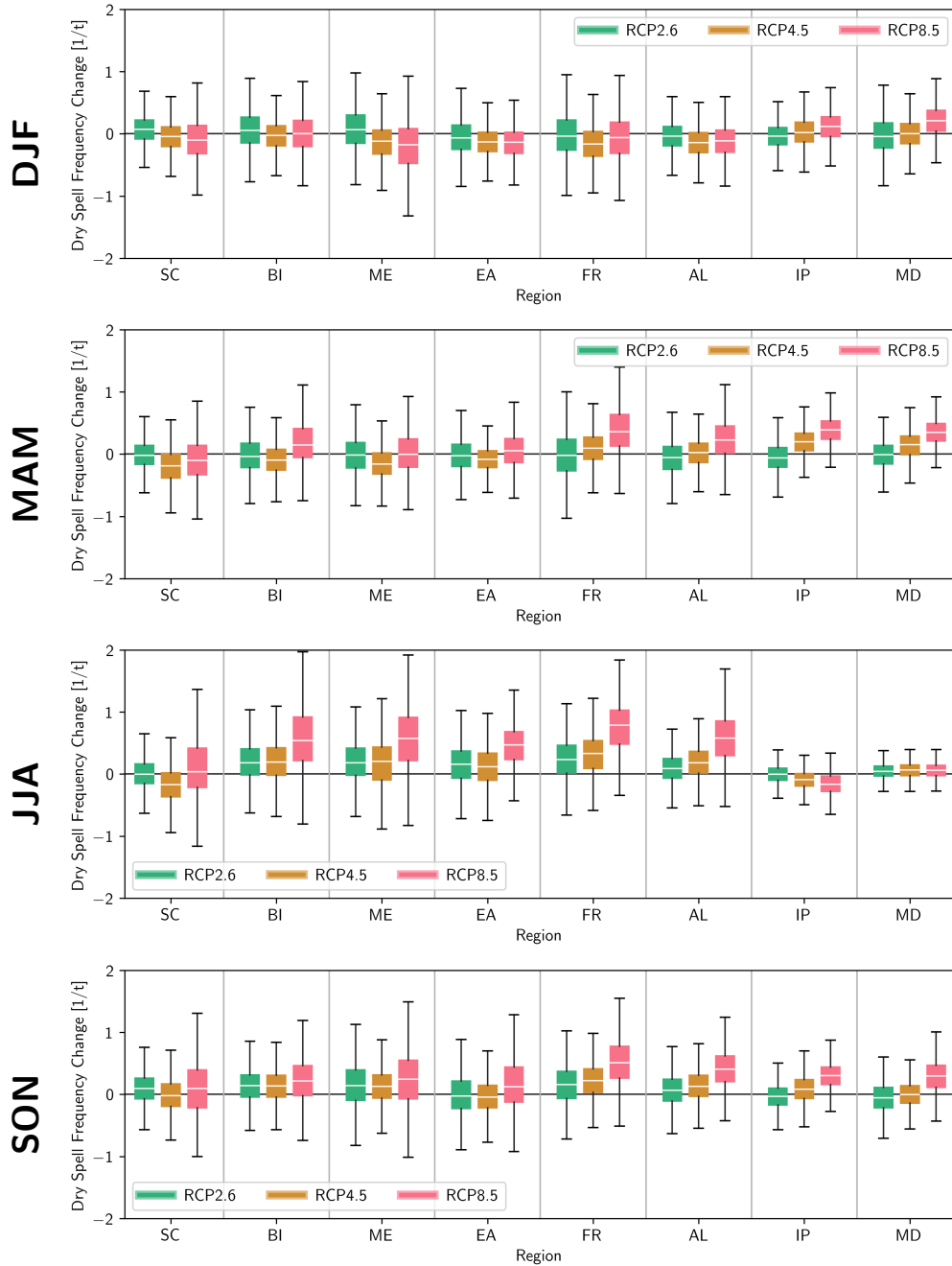
Figure 4.6: Same as Figure 4.5 for frequency of dry spells. A dry spell is defined as an event with at least 7 consecutive days with precipitation below 1 mm per day (see Subsection 2.2).

different return periods (5 a, 10 a, 25 a, 50 a and 100 a) for the 8 regions defined in Figure 2.1. In general Figure 4.7 resembles our previous findings, with no significant changes over most of Europe. Only for Iberian Peninsula and Mediterranean a small increase in the length of drought

events across all return periods is simulated. However these changes develop at global warming levels above 3.0 K. At lower warming levels only a marginal change is visible. Considering the overall change in IP and MD, return periods roughly double between historical conditions and a 4.0 K world, i.e. a 10-year event is becoming a 5-year event (twice as often). However the absolut changes are quite small ($\approx$ 5 days).
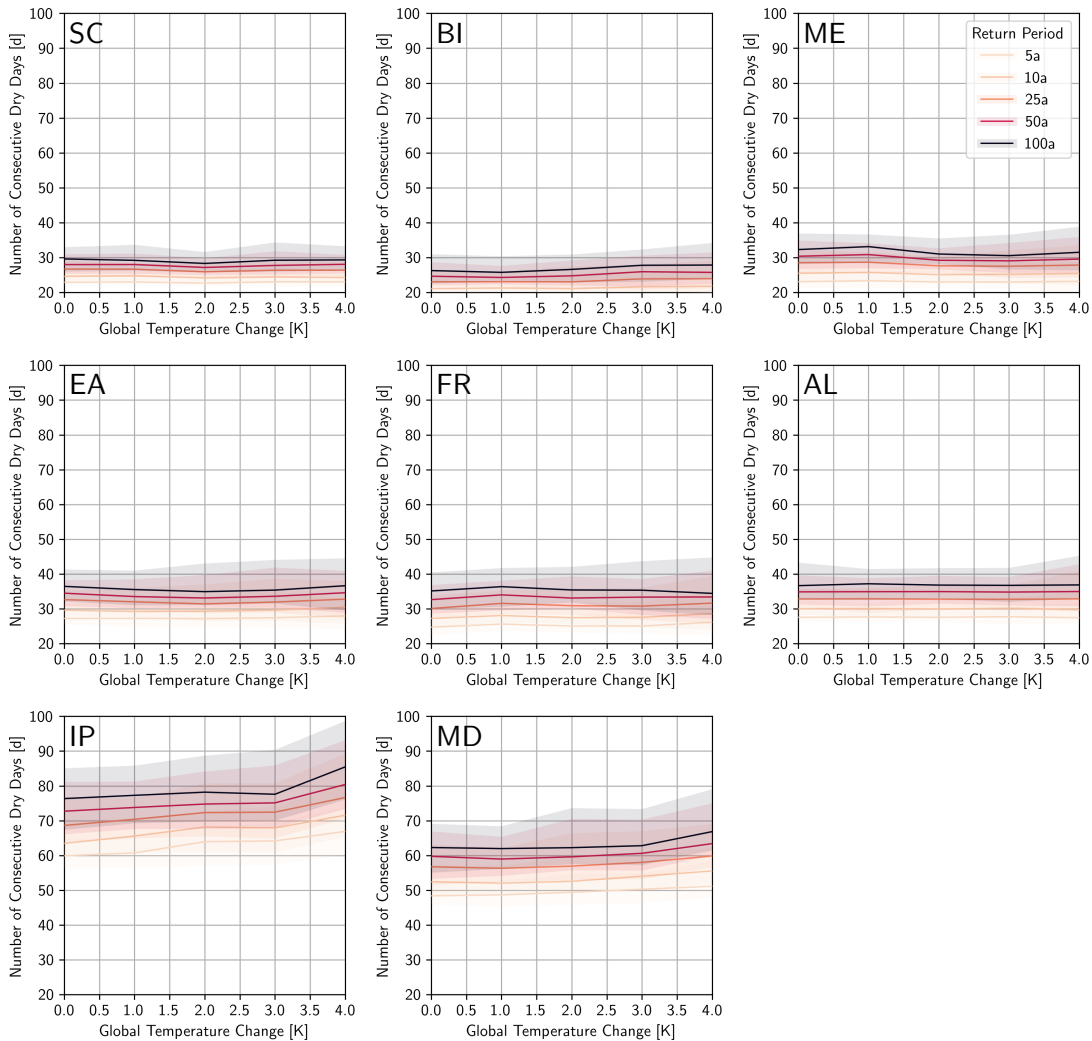

Figure 4.7: Length of drought events with specified return period for different global warming levels. Each plot represents one of the regions defined in Figure 2.1. Each line is based on all CORDEX-EUR11 RCM simulations and greenhouse gas concentration scenarios with each model aligned to the respective CMIP5 GCM global temperature change, with respect to 1981–2010. For each 0.5 K warming level (0.0 K, 0.5 K, 1.0 K, 1.5 K, etc.) a window of 1 K width is used to select years from the GCMs. The maximum drought length for each of these years in the respective RCM simulation were subsequently used to fit a Generalized Extreme Value (GEV) distribution and estimate the length of drought events for a given return period. For the calculations we used the full modeled time period 1981–2100 of the bias adjusted RCM ensemble.

As shown in Figure 4.4, evapotranspiration is anticipated to increase considerable over Europe in all seasons. Therefore, when evaluating the projected change in drought events, one also has to include the effect of evapotranspiration, as it will affect drought severity. To evaluate the impact of a drought on the ecological, hydrological, agricultural, and social systems one also has to consider the time scale over which water deficits accumulate. To include the effect of evapotranspiration on drought severity and time scale on drought type in our evaluation, we utilized the SPEI (see Subsection 2.2). Figure 4.8 shows the changes in SPEI for four different time scales (3, 6, 12 and 24 months) at the end of the 21st century. Similar to the precipitation changes (see Figure 4.3), we found a south to north gradient in SPEI. Most of northern and central Europe is projected to show only a small increase due to the strong precipitation increase unable to be compensated by the moderate increase in evapotranspiration. Furthermore, these changes are below statistical significance. The southern parts of Europe, on the other hand, show a strong decrease in SPEI. These changes are attributed to the decrease in precipitation and increase in temperature, leading to higher evapotranspiration. Considering different time scales from 3 to 24 months these spatial patterns persist. The intensity of decrease over southern Europe however increases with longer time scales. Hence, drought change severity accumulates due to the decreasing precipitation and increasing evapotranspiration throughout the year. Furthermore, the significant increase over all time scales implies, that future drought will substantially affect the whole hydrological cycle at the surface. The projections anticipate, that soil water, river discharge, reservoir and groundwater storages will undergo a significant decrease in southern Europe and this will have a strong impact especially on the agricultural sector.
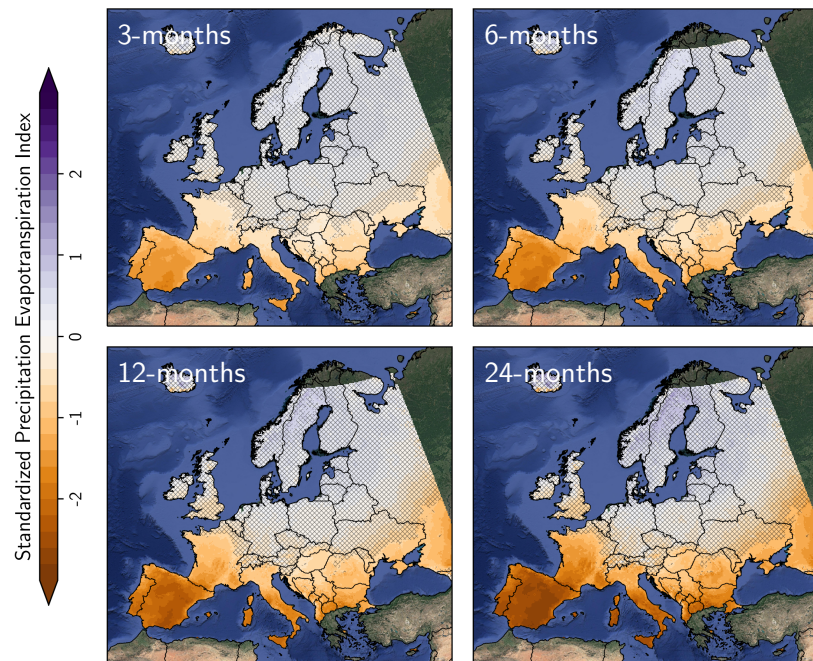

Figure 4.8: Change of SPEI for 4 different time-scales. Changes are calculated for 2071–2100 with respect to 1981–2010 based on the bias adjusted RCM ensemble under concentration scenario RCP 8.5.

For the implementation of measures to adapt or mitigate the negative impacts of anticipated

climate change it is important to have an idea about the timing of these impacts. In other words, we should have a rough estimate of when certain impacts are assumed to emerge. Therefore, Figure 4.9 shows for 4 different SPEI scales and 3 different concentration scenarios the decade at which persistent negative SPEI values starting to emerge, i.e., the decade when SPEI turns from predominantly positive to negative values. In detail, for a running 10-year window we estimated the ensemble 85 percentile time series of SPEI (annual mean for 3-, 6-, 12- and 24-months scale) and identified the year (i.e., center year of the 10-year window) at which this time series crosses 0.0 for the first time. Due to the 10-year window the ensemble 85 percentile time series is already sufficiently smooth. However, there is the possibility that in the following years the time series went back to positive SPEI values. To indicate this time series behavior we shade grid boxes, where more then 15 % of the following years show positive SPEI. Due to construction Figure 4.9 depicts decades in which the climatic conditions of SPEI turns towards persistent dry conditions across the whole ensemble. Individual models and decades can still show significant negative SPEI.

In agreement with our previous findings persistent negative SPEI will develop in the southern parts of Europe first. With increasing greenhouse gas concentrations regions with negative SPEI propagate northward, as temperature and evapotranspiration increases. For a majority of southern regions this change will happen in the first half of the 21st century. The more we move northward, the later the shift will emerge. Under RCP 8.5, the Mediterranean, most parts of France and the Ukraine will experience mostly negative SPEI levels at each time scale. Most of the central European and northern countries, except for the British Isles, do not show a persistent shift across all ensemble members until 2100. Under the low concentration scenario RCP 2.6 only the southernmost areas show a change within the century. Furthermore, the change is not persistent, as more than 15 % of the years after the first appearance of a negative SPEI show positive values, due to a high signal-to-noise ratio. Considering the different time scales of SPEI, we observe a slight northward shift and earlier occurrence of negative SPEI with increasing scale. This finding implies, that shift towards dry conditions will be first observed on systems slowly reacting to changes in the hydrological cycle, like soil and groundwater.
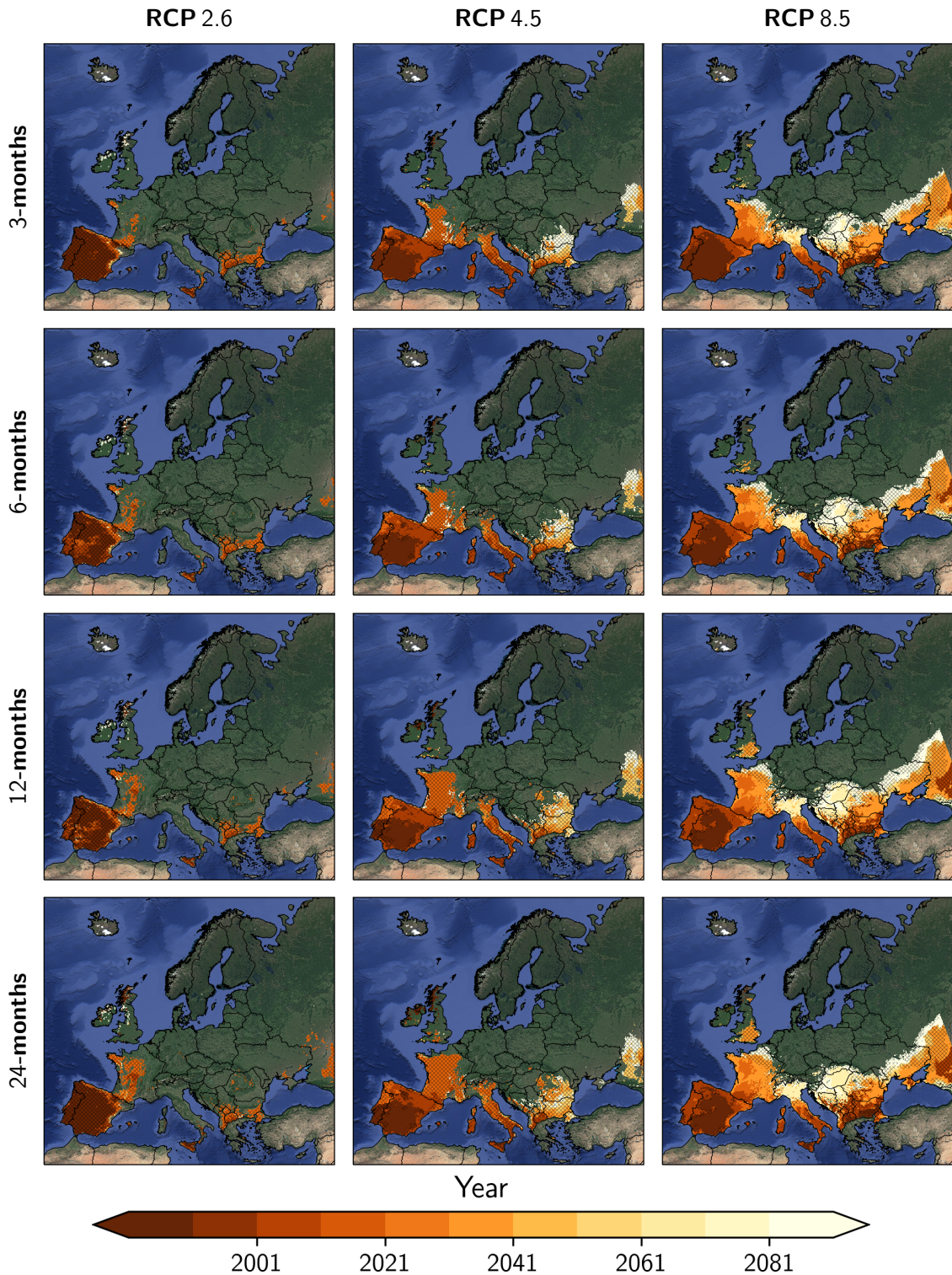
Figure 4.9: Decade when persistent negative values of SPEI are anticipated for different SPEI scales and greenhouse gas concentration scenarios. Based on our RCM ensemble we calculated the 85 percentile for a 10-year running window of annual mean SPEI. The plotted year represent the center of a 10-year window when the 85 percentile time series of SPEI turns negative for the first time. The shaded area depicts regions where more than 15 % of the following years (after SPEI goes negative for the first time) have positive SPEI again, i.e. due to high variability in SPEI time series the negative trend is not persistent.

5 Conclusion

Based on observations from E-OBS v24.0e and bias adjusted RCM projections for CORDEX-EUR11 we investigated the past and projected changes in meteorological droughts for the European continent. From 1981 to 2020 the European continent experienced a wide-spread temperature increase leading to an increase in evapotranspiration. However, due to heterogeneous precipitation change this is only weakly reflected in meteorological drought indices. Our analysis shows, that only central European areas, which are also major agricultural and socio-economic centers of Europe were affected by increased number of dry days and dry spell frequency. Due to the low magnitude of these changes in comparison to the high inter-annual variability of drought events, most historical changes are below statistical significance. The overall strongest drying trends were observed for the agricultural important summer season.

With respect to the anticipated future conditions we found statistical significant changes in all drought related variables for the Mediterranean region. This change is primarily driven by reduced precipitation especially in spring, summer and autumn. Since the Mediterranean is already one of the driest regions in Europe the absolute change in drought length and frequency is quite small until the end of the 21st century even under a high greenhouse gas concentration scenario. However, drought intensity in terms of SPEI is changing considerably. We found a north to south contrast of changes in SPEI with statistical significant increases over the Mediterranean, parts of the Ukraine and France, while only a small and statistical insignificant increase is found for the rest of Europe. This change pattern is primarily driven by temperature changes. As temperature is expected to increase significantly and homogeneously by up to 5.3 K, evapotranspiration will also increase. This increase can only be compensated in regions and seasons with precipitation increase, like over Scandinavia. The Mediterranean on the other hand has to endure both, precipitation decrease and evapotranspiration increase. The anticipated changes will put additional pressure on the important agricultural sector in that region. Our findings show furthermore, that these changes are most likely to emerge within the first half of the 21st century within slowly evolving components of the hydrological cycle, like soil and groundwater.

Surprisingly the already observed climate change over Europe did not show the similar pattern like projected for the future by our RCM ensemble. At the current state it is unknown weather this is due to the short time frame of observations or due to insufficiencies in the models. With respect to the evaluation of the bias adjusted RCM ensemble one can argue, that the models overestimate the intensity of changes in drought events, as we found a small dry bias after bias adjustment. Furthermore, the findings of Boberg and Jens H. Christensen (2012) support this argument for the Mediterranean. This aspect needs to be further studied in the future.

Bibliography

Glahn, Harry R. and Dale A. Lowry (1972). "The Use of Model Output Statistics (MOS) in Objective Weather Forecasting". In: *Journal of Applied Meteorology and Climatology* 11.8, pp. 1203–1211. DOI: 10.1175/1520-0450(1972)011<1203:TUOMOS>2.0.CO;2.

Efron, B. (1979). "Bootstrap Methods: Another Look at the Jackknife". In: *The Annals of Statistics* 7.1, 1–26(26). DOI: 10.1214/aos/1176344552.

Hargreaves, George and Zohrab Samani (Jan. 1985). "Reference Crop Evapotranspiration From Temperature". In: *Applied Engineering in Agriculture* 1. DOI: 10.13031/2013.26773.

Efron, B. and R. Tibshirani (1986). "Bootstrap Methods for Standard Errors, Confidence Intervals, and Other Measures of Statistical Accuracy". In: *Statistical Science* 1.1, 54–75(22). DOI: 10.1214/ss/1177013815.

Allan, Richard, L. Pereira, and Martin Smith (Jan. 1998). *Crop evapotranspiration-Guidelines for computing crop water requirements-FAO Irrigation and drainage paper 56*. Vol. 56.

Gong, D.-Y. and C.-H. Ho (2002). "The Siberian High and climate change over middle to high latitude Asia". In: *Theoretical and Applied Climatology* 72.1, pp. 1–9. ISSN: 1434-4483. DOI: 10.1007/s007040200008.

Christensen, Jens Hesselbjerg and Ole Bøssing Christensen (2007). "A summary of the PRUDENCE model projections of changes in European climate by the end of this century". In: *Climatic Change* 81.1, pp. 7–30. ISSN: 1573-1480. DOI: 10.1007/s10584-006-9210-7.

Christensen, Jens H., Fredrik Boberg, Ole B. Christensen, and Philippe Lucas-Picher (2008). "On the need for bias correction of regional climate change projections of temperature and precipitation". In: *Geophysical Research Letters* 35.20. DOI: 10.1029/2008GL035694.

Vicente-Serrano, Sergio M., Santiago Beguería, and Juan I. López-Moreno (2010). "A Multiscalar Drought Index Sensitive to Global Warming: The Standardized Precipitation Evapotranspiration Index". In: *Journal of Climate* 23.7, pp. 1696–1718. DOI: 10.1175/2009JCLI2909.1.

Dosio, A. and P. Paruolo (2011). "Bias correction of the ENSEMBLES high-resolution climate change projections for use by impact models: Evaluation on the present climate". In: *Journal of Geophysical Research: Atmospheres* 116.D16. DOI: 10.1029/2011JD015934.

van Vuuren, Detlef P., Jae Edmonds, Mikiko Kainuma, Keywan Riahi, Allison Thomson, Kathy Hibbard, George C. Hurtt, Tom Kram, Volker Krey, Jean-Francois Lamarque, Toshihiko Masui, Malte Meinshausen, Nebojsa Nakicenovic, Steven J. Smith, and Steven K. Rose (2011). "The representative concentration pathways: an overview". In: *Climatic Change* 109.1, p. 5. ISSN: 1573-1480. DOI: 10.1007/s10584-011-0148-z.

Boberg, Fredrik and Jens H. Christensen (2012). "Overestimation of Mediterranean summer temperature projections due to model deficiencies". In: *Nature Climate Change* 2.6, pp. 433–436. ISSN: 1758-6798. DOI: 10.1038/nclimate1454.

Teutschbein, Claudia and Jan Seibert (2012). "Bias correction of regional climate model simulations for hydrological climate-change impact studies: Review and evaluation of different methods". In: *Journal of Hydrology* 456-457, pp. 12–29. ISSN: 0022-1694. DOI: 10.1016/j.jhydrol.2012.05.052.

Bellprat, O., S. Kotlarski, D. Lüthi, and C. Schär (2013). "Physical constraints for temperature biases in climate models". In: *Geophysical Research Letters* 40.15, pp. 4042–4047. DOI: 10.1002/grl.50737.

Hempel, S., K. Frieler, L. Warszawski, J. Schewe, and F. Piontek (2013). "A trend-preserving bias correction - the ISI-MIP approach". In: *Earth System Dynamics* 4.2, pp. 219–236. DOI: 10.5194/esd-4-219-2013.

Wilcke, Renate Anna Irma, Thomas Mendlik, and Andreas Gobiet (2013). "Multi-variable error correction of regional climate models". In: *Climatic Change* 120.4, pp. 871–887. ISSN: 1573-1480. DOI: 10.1007/s10584-013-0845-x.

Jacob, Daniela, Juliane Petersen, Bastian Eggert, Antoinette Alias, Ole Bøssing Christensen, Laurens M. Bouwer, Alain Braun, Augustin Colette, Michel Déqué, Goran Georgievski, Elena Georgopoulou, Andreas Gobiet, Laurent Menut, Grigory Nikulin, Andreas Haensler, Nils Hempelmann, Colin Jones, Klaus Keuler, Sari Kovats, Nico Kröner, Sven Kotlarski, Arne Kriegsmann, Eric Martin, Erik van Meijgaard, Christopher Moseley, Susanne Pfeifer, Swantje Preuschmann, Christine Radermacher, Kai Radtke, Diana Rechid, Mark Rounsevell, Patrick Samuelsson, Samuel Somot, Jean-Francois Soussana, Claas Teichmann, Riccardo Valentini, Robert Vautard, Björn Weber, and Pascal Yiou (2014). "EURO-CORDEX: new high-resolution climate change projections for European impact research". In: *Regional Environmental Change* 14.2, pp. 563–578. ISSN: 1436-378X. DOI: 10.1007/s10113-013-0499-2.

Kotlarski, S., K. Keuler, O. B. Christensen, A. Colette, M. Déqué, A. Gobiet, K. Goergen, D. Jacob, D. Lüthi, E. van Meijgaard, G. Nikulin, C. Schär, C. Teichmann, R. Vautard, K. Warrach-Sagi, and V. Wulfmeyer (2014). "Regional climate modeling on European scales: a joint standard evaluation of the EURO-CORDEX RCM ensemble". In: *Geoscientific Model Development* 7.4, pp. 1297–1333. DOI: 10.5194/gmd-7-1297-2014.

Cannon, Alex J., Stephen R. Sobie, and Trevor Q. Murdock (2015). "Bias Correction of GCM Precipitation by Quantile Mapping: How Well Do Methods Preserve Changes in Quantiles and Extremes?" In: *Journal of Climate* 28.17, pp. 6938–6959. DOI: 10.1175/JCLI-D-14-00754.1.

Li, Fei and Yong-Qi Gao (2015). "The Project Siberian High in CMIP5 Models". In: *Atmospheric and Oceanic Science Letters* 8.4, pp. 179–184. DOI: 10.3878/AOSL20140101.

Maraun, Douglas (2016). "Bias Correcting Climate Change Simulations - a Critical Review". In: *Current Climate Change Reports* 2.4, pp. 211–220. ISSN: 2198-6061. DOI: 10.1007/s40641-016-0050-x.

Lange, Stefan (Dec. 2017). *ISIMIP2b Bias-Correction Code*. DOI: 10.5281/zenodo.1069050.

Cornes, Richard C., Gerard van der Schrier, Else J. M. van den Besselaar, and Philip D. Jones (2018). "An Ensemble Version of the E-OBS Temperature and Precipitation Data Sets". In: *Journal of Geophysical Research: Atmospheres* 123.17, pp. 9391–9409. DOI: 10.1029/2017JD028200.

Hanel, Martin, Oldich Rakovec, Yannis Markonis, Petr Máca, Luis Samaniego, Jan Kyselý, and Rohini Kumar (2018). "Revisiting the recent European droughts from a long-term perspective". In: *Scientific Reports* 8.1, p. 9499. ISSN: 2045-2322.

Spinoni, Jonathan, Jürgen V. Vogt, Gustavo Naumann, Paulo Barbosa, and Alessandro Dosio (2018). "Will drought events become more frequent and severe in Europe?" In: *International Journal of Climatology* 38.4, pp. 1718–1736. DOI: 10.1002/joc.5291.

García-Herrera, Ricardo, Jose M. Garrido-Perez, David Barriopedro, Carlos Ordóñez, Sergio M. Vicente-Serrano, Raquel Nieto, Luis Gimeno, Rogert Sorí, and Pascal Yiou (2019). "The

European 2016/17 Drought". In: *Journal of Climate* 32.11, pp. 3169–3187. DOI: `https://doi.org/10.1175/JCLI-D-18-0331.1`.

Lange, Stefan (2019). "Trend-preserving bias adjustment and statistical downscaling with ISIMIP3BASD (v1.0)". In: *Geoscientific Model Development* 12.7, pp. 3055–3070. DOI: `10.5194/gmd-12-3055-2019`.

Commission, European, Joint Research Centre, C Cammalleri, G Naumann, L Mentaschi, G Formetta, G Forzieri, S Gosling, B Bisselink, A De Roo, and L Feyen (2020). *Global warming and drought impacts in the EU : JRC PESETA IV project : Task 7*. Publications Office. DOI: `doi/10.2760/597045`.

MedECC (Nov. 2020). *Climate and Environmental Change in the Mediterranean Basin Current Situation and Risks for the Future. First Mediterranean Assessment Report*. Version 1. Preferred citation: MedECC (2020) Climate and Environmental Change in the Mediterranean Basin Current Situation and Risks for the Future. First Mediterranean Assessment Report [Cramer, W., Guiot, J., Marini, K. (eds.)]. Union for the Mediterranean, Plan Bleu, UNEP/MAP, Marseille, France, 632 pp., ISBN: 978-2-9577416-0-1, doi:10.5281/zenodo.4768833. DOI: `10.5281/zenodo.4768833`.

Commission, European, Joint Research Centre, P Barbosa, D Masante, C Arias Muñoz, C Cammalleri, A De Jager, D Magni, M Mazzeschi, N McCormick, G Naumann, J Spinoni, and J Vogt (2021). *Droughts in Europe and worldwide 2019-2020*. Publications Office. DOI: `doi/10.2760/415204`.

Rakovec, Oldrich, Luis Samaniego, Vittal Hari, Yannis Markonis, Vojtch Moravec, Stephan Thober, Martin Hanel, and Rohini Kumar (2022). "The 20182020 Multi-Year Drought Sets a New Benchmark in Europe". In: *Earth's Future* 10.3. e2021EF002394 2021EF002394, e2021EF002394. DOI: `https://doi.org/10.1029/2021EF002394`.

Acronyms

BASD Bias Adjustment and Statistical Downscaling

CMIP Coupled Model Intercomparison Project

CORDEX Coordinated Regional Climate Downscaling Experiment

FAO Food and Agriculture Organization

GCM Global Climate Model

GEV Generalized Extreme Value

ISIMIP3 The Inter-Sectoral Impact Model Intercomparison Project Phase 3

RCM Regional Climate Model

RCP Representative Concentration Pathway

SPEI Standardized Precipitation Evapotranspiration Index

TOA top-of-the-atmosphere

DJF December-January-Februar

MAM March-April-May

JJA June-July-August

SON September-October-November

AL Alps

BI British Isles

EA Eastern Europe

FR France

IP Iberian Peninsula

ME Mid-Europe

MD Mediterranean

SC Scandinavia